



Calcite twins from microveins as indicators of deformation history

José M. González-Casado^{a,*}, Carmen García-Cuevas^b

^a*Departamento de Q. A. Geología y Geoquímica, Facultad de Ciencias, Universidad Autónoma de Madrid, 28049 Madrid, Spain*

^b*Departamento de Geodinámica, Facultad Ciencias Geológicas, Universidad Complutense, 28040 Madrid, Spain*

Received 24 November 1997; accepted 22 February 1999

Abstract

In order to investigate whether the evidence of the deformation history is preserved in the microvein calcite twinning microstructures, several families of calcite veins have been studied from weakly deformed mesozoic limestones of the western Iberian Chain (eastern Iberian Peninsula). The maximum shortening directions established with this method correspond to the previously established paleostress evolution of this chain. The reconstructed stress regimes evolve from predominantly compressional (four compressional episodes, with the maximum shortening direction oriented successively NW–SE, N–S, NE–SW and E–W) to extensional. The established orientations of maximum shortening axes are consistent with the directions of paleostrains that have been independently deduced from stylolites and fault striations in the same region. Moreover, the results clearly show that the e-twins record some paleostress orientations that are not registered in the studied area by fault population analysis. In this sense, the e-twins record older paleostress orientations than the small faults, probably because the faults were reactivated several times and the twins were not modified since their formation. The calculated values of twin strains, ~1%; differential stress magnitudes, 62 MPa; and the existence of type I twins formed below 200°C, confirm that this region was slightly deformed under low *P–T* conditions. © 1999 Elsevier Science Ltd. All rights reserved.

1. Introduction

Several methods of strain and stress analysis have been developed using calcite e-twin data (e.g. Turner, 1953, 1962; Weiss, 1954; Turner and Weiss, 1963; Groshong, 1972, 1974, 1988; Spang, 1972; Jamison and Spang, 1976; Groshong et al., 1984a; Rowe and Rutter, 1990; Ferrill, 1991, 1998; Burkhard, 1993; Evans and Groshong, 1994; Newman, 1994; Lacombe and Laurent, 1996). These methods are based on the fact that at low pressure and temperature, calcite aggregates deform primarily by e-twinning. Some of these allow the complete (principal axes orientations and relative magnitudes) or partial (only principal axes orientations) strain–stress tensor to be determined, whereas the other established only paleodifferential

stress magnitudes (paleopiezometers) based on twin density (e.g. Rowe and Rutter, 1990) or on the percentage of carbonate grains with one, two, or three twin sets (e.g. Jamison and Spang, 1976). The conclusions obtained from application of these methods are in general difficult to draw when twins were not formed under a single stress field, or were passively rotated after formation. The development of twins under non-coaxial conditions also complicates the interpretation, although, the very small strains that results from twinning can usually be approximated by coaxial conditions.

The simplest methods are based on the fact that the movement on twins can take place in only one direction, and the *c*-axes in the twin lamellae and in the host are related by a fixed angle. By measuring the orientation of the twin planes and the *c*-axes, the directions of ‘compression’ (*C*) and ‘tension’ (*T*) responsible for the twinning can be deduced (Turner, 1953, 1962; Weiss, 1954).

* Corresponding author.

E-mail address: G.Casado@uam.es (J.M. González-Casado)

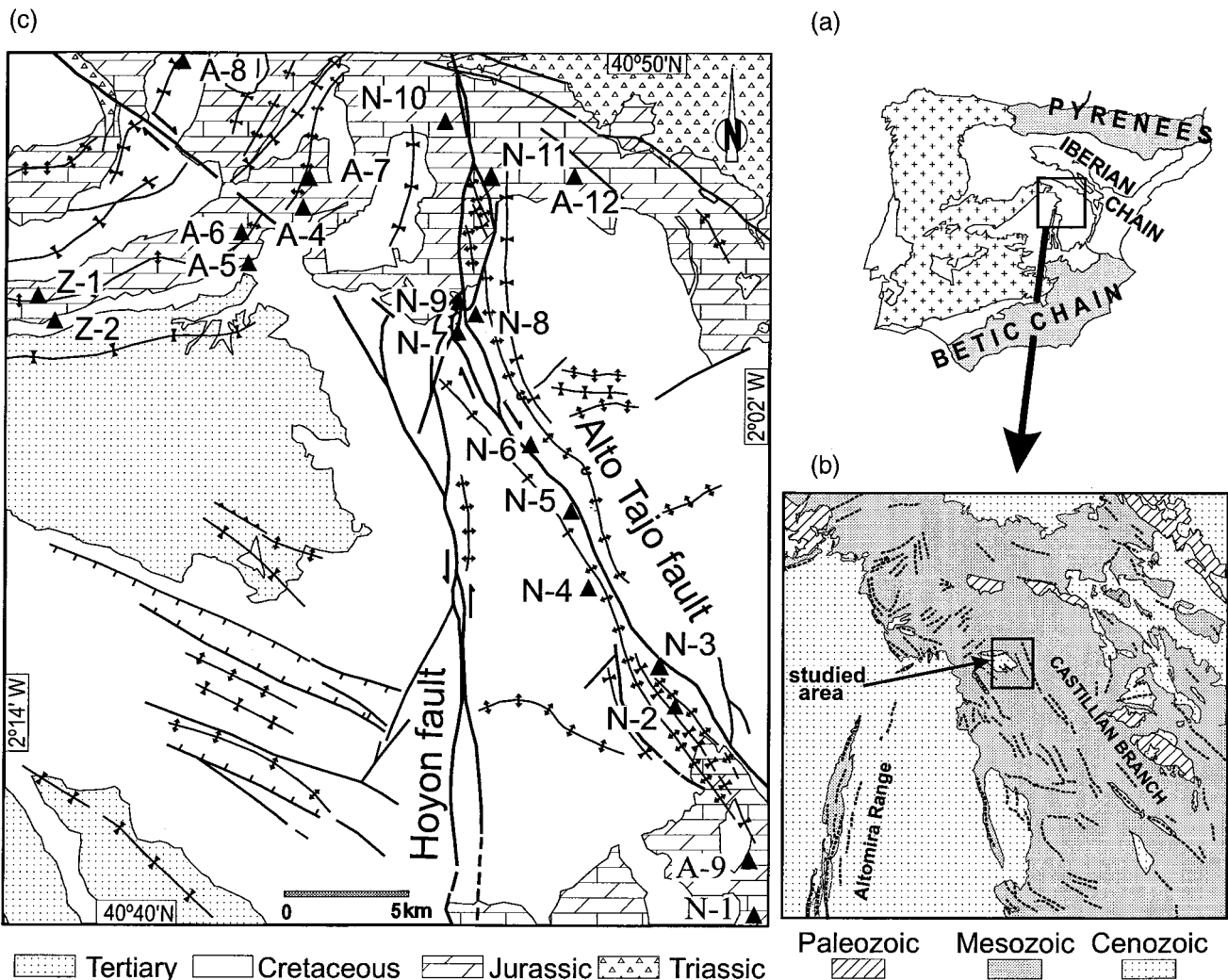


Fig. 1. (a) Location of the Iberian Chain and its surrounding tectonic units within the Iberian Peninsula. (b) Location of the studied area in the Castilian Branch of the Iberian Chain. Dashed lines represent fold trends. (c) Geological sketch of the Sierra del Alto Tajo (NW Iberian Chain), showing the location of the main structures and sampling stations (the figure is based in part on: Adell et al., 1981, I.G.M.E. Geological Map No 513 and Rodríguez-Pascua et al., 1994).

This technique may be extended to yield strain information associated with the twinning by measuring the number and average thickness of the twins, where the amount of simple shear deformation in any twinned crystal is directly proportional to the thickness of the twinned portion in the crystal. The relative percentage of twinned portion of each grain is taken into account and a value of the shear strain produced by the twinning is obtained for each twin set. A complete strain tensor for the sample is calculated by means of a least-square technique, which accounts for a maximum of twins (Groshong, 1972, 1974; Groshong et al., 1984b; Evans and Groshong, 1994). Grains that are not properly oriented for twinning with respect to this tensor are identified by calculating the value of the strain in each twin set and the deviation of this strain from the complete strain tensor. The incompatible twin sets

yield so-called negative expected values (NEV) of strain and may indicate one or more of: grain measurement errors, errors in the calculation of the principal strain axes, heterogeneous strain (at grain or sample scale), non-coaxial deformation and superimposed deformation. The fit of the calculated strain tensor to the data may be improved by eliminating the incompatible twin sets that give the largest deviation (NEVs). These values can be discarded as noise (Groshong, 1972; Groshong et al., 1984a) or be used to run a new analysis. In some cases, this second possibility permits different strain tensors, i.e. superimposed deformations, to be identified (Teufel, 1980; Laurent et al., 1981; Lacombe et al., 1990).

In limestones deformed at low P - T conditions, the grains that are most likely to be twinned are the coarse sparitic crystals, which are found in the pore-filling

cement. However, when the volume fraction of pore-filling cement is small, or when the rock is so weakly strained that only a very few grains are twinned, it is difficult to find a statistically sufficient number of twinned grains to carry out the stress and strain analyses. Nevertheless, these rocks often contain small veins filled with sparry calcite crystals. The aim of the present study is to analyse the e-twins of these micro-veins and to establish whether they can be used to determine the geometry of successive deformation events occurring after the growth of the vein. In order to test the validity of the method, we have compared the results obtained from the calcite e-twin analysis to those that were deduced from employing other stress indicators, e.g. fault slip data and stylolite orientations (Lacombe et al., 1992; Rocher et al., 1996). In order that these alternative stress indicators could be used in this way, the samples for this analysis have been taken from the western side of the Iberian Chain (Celtiberian Chain, eastern Iberian Peninsula, Fig. 1), where stress history during the Cenozoic has been well established from small and major structures.

2. Geological setting

The Iberian Chain is a straight NW–SE-trending fold and thrust belt located between the Ebro, Duero and Tajo Tertiary basins, in the eastern part of the Iberian Peninsula (Fig. 1a). This is an intraplate chain built up mainly during the Paleogene in response to the compressional tectonics then occurring on the active margins of the Iberian Plate in the Pyrenees and the Betic Cordillera. Subsequently, from the Upper Neogene to the present-day, the region has been extending. This mountain range is made of a thick cover of Jurassic and Cretaceous sedimentary rocks overlying Germanic facies Triassic material. The Lower Triassic sediments lie on an erosional surface, which truncates the metamorphic Palaeozoic rocks of the Hercynian basement. The Mesozoic sedimentary sequence was deposited during several episodes of rifting and thermal subsidence, and attains thicknesses of over 1500 m (Alvaro et al., 1979; Vilas et al., 1983; Salas and Casas, 1993). In the Iberian Chain, there are two main directions of major compressional structures, one subparallel to the longitudinal trend of the chain (NW–SE folds and reverse faults) and the other transverse to it (NE–SW). Locally, in this region are found folds with a N–S orientation (Altomira Range, Fig. 1b).

The Sierra del Alto Tajo, where this work is located (Fig. 1b), belongs to the Castillian Branch of the Iberian Chain (western limit). This region comprises flat-lying beds disturbed by gentle folds which trend NW–SE and NE–SW. Associated with some of the

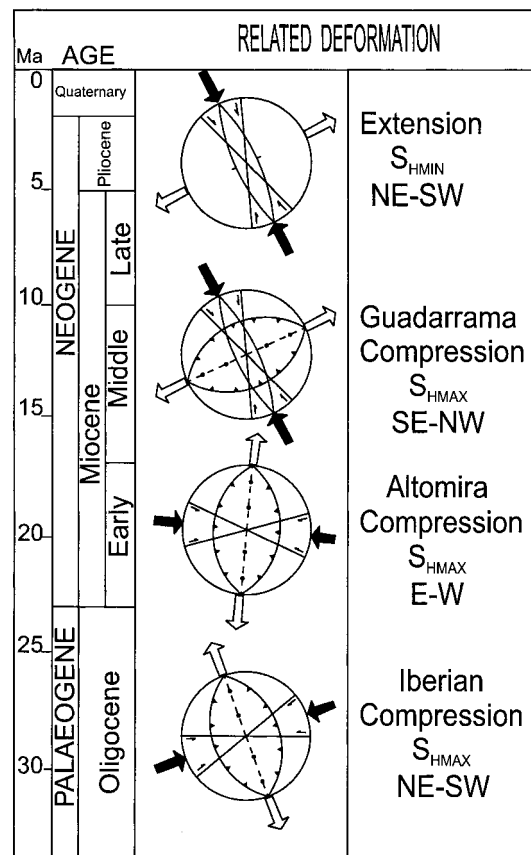


Fig. 2. Sketch of the gradual change in the orientations of the maximum horizontal shortening directions (S_{HMAX} , black arrows) and the maximum horizontal extension direction (white arrows) between the Oligocene and the Pliocene, within the western Iberian Chain. The orientations of the main active structures (faults and folds) associated with each tectonic event are also shown in the stereographic diagrams (the figure is based in part on Muñoz-Martín, 1997).

synformal structures of both fold families, are small sedimentary basins (Fig. 1c) filled with Tertiary continental clastic and lacustrine deposits. Two major strike-slip faults are located in this Sierra: the Alto Tajo fault with a NW–SE-trend and a dextral sense of movement (Fig. 1c), and the Hoyon fault, with a N–S orientation (Fig. 1c) and a sinistral displacement. The displacements of these faults gave rise to the development of other structures including folds, strike-slip duplexes and small positive flower structures (Rodríguez-Pascua et al., 1994).

The Tertiary sedimentary record (Calvo et al., 1993) and the previous microstructural studies carried out in this part of the Iberian Chain show that the Cenozoic evolution of this area has involved polyphase deformation (e.g. Alvaro, 1975; Manera, 1981; Capote et al., 1982; Simón-Gómez, 1986; De Vicente, 1988; Capote et al., 1990; De Vicente et al., 1992, 1996; Rodríguez-Pascua, 1993; Muñoz-Martín, 1997). The principal deformation events, clearly separated in time,

during the development of the Iberian Chain were (Fig. 2):

1. Iberica Compression (IC). NE–SW directed shortening during the Eocene (?) and Oligocene, probably in response to compression in the Pyrenean margin of the Iberian plate (Simón-Gómez, 1986).
2. Altomira Compression (AC). A local episode of shortening visible only in the Sierra de Altomira (western border of the Castillian Branch, Fig. 1a). The observed E–W shortening direction probably resulted from a superposition of the shortening occurring on the Pyrenean margin with that beginning in the Betic tectonic margin (Muñoz-Martín et al., 1994; Muñoz-Martín, 1997).
3. Guadarrama Compression (GC). Forms the major structures of this area (Iberian Chain and Spanish Central System, Fig. 1) and corresponds to a new compressional episode that took place from the Middle to the Upper Miocene (De Vicente, 1988; Capote et al., 1990; De Vicente et al., 1992; Sell et al., 1995; De Vicente et al., 1996). In this event, the maximum horizontal shortening direction (S_{HMAX}) was oriented NW–SE. The shortening was probably connected to the continental deformation of the Betic Chain after the end of the Pyrenean activity.
4. After these compressional events, the microstructural analysis records a strong NE–SW extensional episode, which occurred between the Pliocene and the present day. During this extension, many of the previous NW–SE faults were reactivated as normal faults. Also, small extensional basins were created. This extension has been attributed to the delayed propagation, towards the interior of Iberia, of the extension associated with the opening of the Valencia Trough in the Neogene (De Vicente et al., 1996).

3. Methods used for strain and stress analysis

In order to investigate the evidence of the deformation history of the area that is preserved in the calcite microvein twinning microstructures, 20 oriented samples of limestones (mudstones and grainstones) were collected from the Lower Jurassic and Upper Cretaceous units (Fig. 1c). Analysis of the twinning microstructures in the pore-filling calcite cement of the host rocks was also carried out on three samples (N3, N6 and N7) for comparison with the results obtained from microveins.

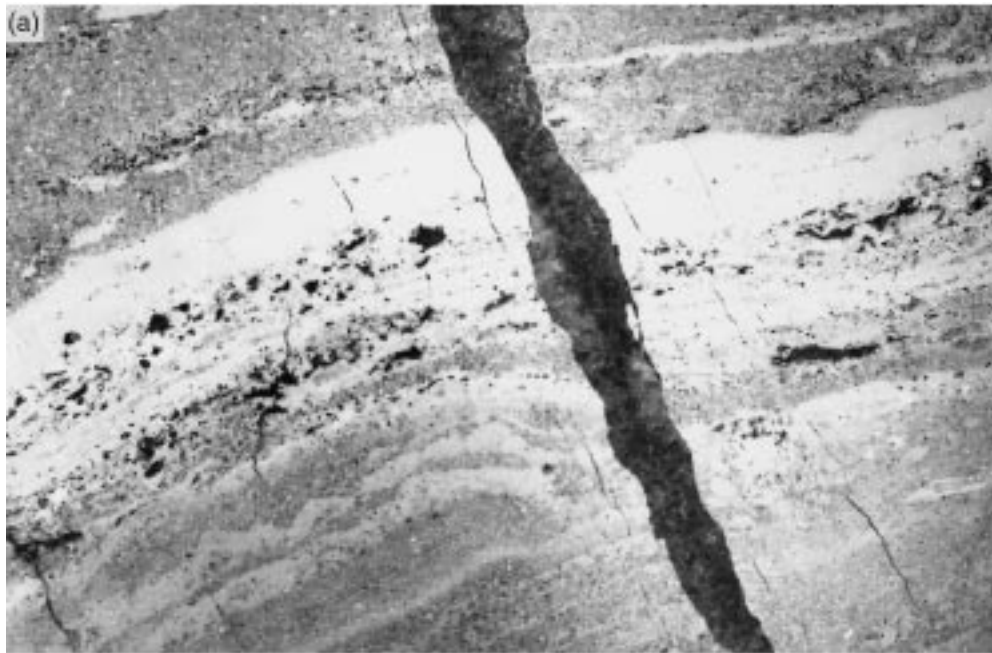
Each microstructural analysis was carried out using a standard optical polarizing microscope equipped with a universal stage. For each sample, measurements

were made on two orthogonal thin sections in order to avoid the U-stage ‘blind spot’. About 50 grains were measured on each section, with the following parameters determined for each grain: *c*-axes of host and twin lamellae, twin set orientation, twins’ average thickness, number of twins and grain width.

The strain due to twinning was calculated using the ‘calcite strain-gauge technique’ of Groshong (see Groshong, 1972, 1974, for a detailed description of this analysis method). This technique has been shown by several workers to yield good estimates of the magnitude and orientation of the principal strains in slightly to moderately deformed limestones (e.g. Groshong et al., 1984a; Ferrill, 1991; Burkhard, 1993). The data were analysed using the computer program developed by Evans and Groshong (1994). The program calculates principal strain orientations and magnitudes, total strain due to twinning (square root of second invariant of strain, $\sqrt{(J2)}$), standard errors for the strains, twin density (twins/mm), average twin-width and percent of NEVs. The scatter of the data was reduced by eliminating the 20% of the twin sets which had the largest deviations from calculated expected values (Groshong et al., 1984a). Although the eliminated data could be used to run a new analysis in order to detect superimposed deformations (Teufel, 1980), in this work these twin sets were discarded.

The orientation of the principal stress axes were obtained by using the orientation measurements of the twin plane and the host and twin *c*-axes to calculate the ‘compression’ and ‘tension’ directions for each measured grain, and then by contouring the results obtained from all the grains measured in the given sample on an equal area stereographic projection (Turner, 1953, 1962; Weiss, 1954; Pfiffner and Burkhard, 1987). The calculated principal stress orientations represent deformation events subsequent to the vein development; however, the extension direction during the vein formation episode was established by means of calcite *c*-axes distribution in each sample.

In order to compare the results obtained from calcite analysis (strain tensors and stress axes orientations) with independent methods of estimating the orientation of the principal stresses, we have calculated the stress tensor at the same sites and in their surroundings by means of fault population analysis methods. These procedures are based upon the minimisation of the angles between measured and theoretical striations. The orientation of the theoretical striations is calculated assuming that the slip along the fault takes place in the direction of the maximum resolved shear stress (Bott, 1959), then an hypothetical stress tensor that fits the slip of the maximum number of measured striations with a minimum misfit is established. The fault population analysis method employed here to deduce the paleostress tensor is the ‘stress



 10 mm




 0.2 mm

Fig. 3. Examples of vein geometries. (a) Vein wall, with a straight form and a minor dextral displacement. Parallel polars (PPL). (b) Vein filled with large sparry calcite crystals. The medial suture and two sets of twins in some grains are clearly visible.

inversion method' developed by Reches (1987; Reches et al., 1992). Like other methods of stress analysis it relies on Bott's equation (Bott, 1959): $\tan \theta = n/lm[m^2 - (l - n^2)R]$ where, θ is the theoretical striation pitch on the fault plane, $R = (\sigma_z - \sigma_x)/(\sigma_y - \sigma_x)$, σ_z is vertical principal stress and $\sigma_y > \sigma_x$ are horizontal principal stresses and, l, m, n are the fault directional cosines. In this procedure it also assumes the Navier–Coulomb rupture principle, wherein the fault only slips if it satisfies the failure condition $\tau = c + \mu\sigma_n$, where τ is the shear stress, σ_n is the normal stress, c is the cohesion and μ is the coefficient of friction. The results of Reches's method are presented as the orientation and the relative magnitude of the principal stresses [where $\phi = (\sigma_2 - \sigma_3)/(\sigma_1 - \sigma_3)$] and the calculated coefficient of friction. To use this method, strike, dip, pitch of the striation, and sense of movement were determined for each fault.

Lastly, the maximum shortening direction has also been established at some sites by measuring the orientation of stylolites (Arthaud and Choukroune, 1972), where it is assumed that stylolite columns form parallel to e_3 .

4. Results

The microveins range in thickness from 0.5 to 5 mm and are straight-sided (Fig. 3a). They are approximately vertical but have three main trends of 010°, 100° and 120°. The veins are filled with large sparitic crystals with the grain size average varying between 238 and 1012 μm . The shape of calcite crystals varies from moderately elongate (length/width ratio of grains < 10) to blocky. The existence of medial sutures suggests syntaxial crystal growth (Fig. 3b). Generally, the calcite c -axes are not oriented normal to the vein borders and the opening trajectories deduced from originally adjacent points on the opposite vein walls are also oblique. Consequently, it is inferred that the veins lie at a high angle to the extension directions.

The distribution of c -axes gives four maxima that reflect the changing orientation of the extension direction during the successive episodes of vein crystallisation. These maxima are oriented subhorizontal and show four different trends: N–S (samples A4, A7, A8, A9, A12, N6, N7, N8, N10a and Z1); NE–SW (samples, N2, N5, N9a, N9b and N10b); NW–SE (samples N1, N3 and N11) and E–W (N4 and Z2) (see Fig. 5a–e). Comparing these orientations with the proposed stress evolution through the Cenozoic in this region (Fig. 2), the deduced N–S, NE–SW and NW–SE opening directions are oriented perpendicular to the maximum shortening directions established for the three main compressional episodes described for this region (Altomira, Guadarrama and Ibérica, tectonic

Table 1

The stress tensor calculated for each location using the method of Reches (1987) for analysing fault slip data. N is the total number of faults and n the number of faults used to define the stress tensor. The orientations of the principal stress axes are given as plunge–plunge direction. ϕ describes the relative magnitudes of the principal stresses and μ is the coefficient of friction calculated in the analysis

Site	n/N	Orientation of the principal stresses			ϕ $(\sigma_2 - \sigma_3)/(\sigma_1 - \sigma_3)$	μ
		σ_1	σ_2	σ_3		
N-1	5/5	20/346	68/145	05/253	0.12	0.9
N-2	33/54	29/335	58/135	08/240	0.37	0.8
	14/21	51/135	11/240	36/339	0.11	0.7
N-3	16/26	88/255	01/084	0/354	0.14	0.7
N-4	12/12	02/172	76/072	13/263	0.1	0.7
	33/44	85/056	01/168	04/258	0.42	1.2
N-5	12/23	80/329	09/142	01/232	0.5	0.6
	5/11	42/235	42/021	17/128	0.5	0.5
N-6	5/5	38/020	50/210	05/114	0.27	0.8
N-7	8/9	41/336	46/180	17/077	0.45	0.6
N-9	8/43	57/024	24/161	19/260	0.26	0.9
	19/35	01/349	86/237	03/079	0.42	0.5
N-10	16/41	73/107	11/331	10/239	0.48	0.5
	12/31	06/184	51/283	037/089	0.16	0.02
N-11	5/17	20/184	67/342	07/091	0.34	0.6
	7/12	33/113	42/240	29/001	0.16	0.5
A-4	19/40	69/162	19/322	06/054	0.47	0.6
	7/21	26/092	57/310	16/191	0.29	0.9
A-5	4/12	79/016	10/200	00/110	0.36	0.6
A-6	14/24	66/124	18/342	13/247	0.04	1
A-7	8/10	89/075	00/208	00/298	0.45	0.8
A-8	16/21	12/150	73/293	09/058	0.47	0.8
	5/5	64/029	22/240	12/145	0.7	0.7
A-9	13/27	19/346	18/249	62/119	0.13	0.9
	8/14	67/344	01/249	22/158	0.28	1
A-10	6/6	60/104	19/233	21/331	0.69	0.4
Z-7	11/18	24/008	63/167	08/274	0.26	0.6
Z-8	4/4	53/309	33/101	13/201	0.38	0.7

events). Only the E–W maximum is not related to any compressive stress tensor. Nevertheless, an E–W extension is found in this area associated with the Pliocene extensional regime and it is also visible in the fault analysis (Fig. 6b and Table 1). These correlations suggest that there were several vein growth episodes along the Tertiary, probably related with the main tectonic events.

4.1. Vein strain analysis (twin strain)

Only a small fraction of the calcite grains in the veins are twinned. In addition, the twinned grains are found to be randomly distributed throughout the vein (Fig. 3b). By their appearance, they are classified as type I twins (cf. Weiss, 1954; Ferrill, 1991), suggesting deformation at low temperatures and to only very small strains.

The results of the calcite e-twin analyses in each of the sites are shown in Table 2. As a measure of the

Table 2

Results of calcite e-twin analysis (Groshong's calcite strain-gauge technique). N is the number of measured twins and n the number of twins analysed after removing those with large NEV. Width is the mean twin width, in microns. Density is the twin density (twins/mm). $\sqrt{(J2)}$ is the square root of the second invariant of the strain tensor (percent strain). e_1 , e_2 and e_3 refer to percent elongation and orientation (plunge and plunge azimuth) of maximum (e_1), intermediate (e_2) and minimum (e_3) elongation direction

Sample	N/n	Width (μm)	Density	$\sqrt{(J2)}$	Principal strains (percent elongation)			Standard 'error'
					e_1	e_2	e_3	
N1	49/40	0.47	20.58	0.665	15/273 (0.667)	74/073 (−0.003)	05/182 (−0.664)	0.201
N2	48/39	0.25	27.45	0.394	12/056 (0.482)	60/304 (0.239)	27/152 (−0.721)	0.184
N3	39/32	0.13	13.05	0.080	22/138 (0.146)	22/039 (0.021)	57/268 (−0.167)	0.038
N4	46/37	0.13	8.99	0.119	18/266 (0.042)	49/020 (0.002)	34/163 (−0.045)	0.009
N5	56/45	0.32	19.87	0.424	20/254 (0.562)	04/163 (0.142)	70/062 (−0.704)	0.139
N6	34/28	0.41	9.02	0.271	05/096 (0.898)	62/356 (0.184)	27/188 (−0.714)	0.718
N7	63/51	0.14	16.81	0.11	36/072 (0.091)	43/260 (0.04)	24/322 (−0.132)	0.042
N8	25/20	0.32	9.09	1.792	47/002 (1.723)	24/121 (0.132)	33/228 (−1.854)	1.072
N9a	66/53	1.22	31.26	2.268	18/233 (2.604)	62/103 (0.211)	19/330 (−2.815)	0.618
N9b	57/46	1.00	36.39	3.611	29/045 (3.346)	58/202 (0.481)	10/309 (−3.828)	0.595
N10a	42/34	0.46	57.07	1.600	39/040 (1.705)	49/203 (−0.238)	09/303 (−1.467)	0.714
N10b	66/53	0.82	30.64	1.463	74/086 (1.514)	15/270 (−0.05)	01/180 (−1.464)	0.396
N11	62/50	0.87	14.77	0.450	01/139 (0.563)	73/046 (−0.187)	16/229 (−0.377)	0.221
A4	39/32	0.17	24.2	0.175	47/011 (0.224)	42/179 (0.023)	06/274 (−0.247)	0.131
A7	52/42	0.62	43.13	1.669	23/172 (2.146)	15/269 (−0.408)	69/031 (−1.738)	1.00
A8	39/32	0.25	57.65	0.849	15/358 (0.512)	68/221 (0.181)	13/092 (−0.694)	0.202
A9	38/31	0.14	9.71	0.088	42/334 (0.099)	47/142 (−0.03)	06/238 (−0.069)	0.028
A12	62/50	0.12	17.06	0.084	49/018 (0.084)	28/148 (−0.024)	25/253 (−0.06)	0.033
Z1	46/37	0.27	39.57	0.702	03/170 (0.634)	33/077 (0.121)	57/264 (−0.755)	0.296
Z2	33/27	0.24	32.12	0.471	18/082 (0.524)	08/350 (−0.139)	70/235 (−0.385)	0.233

total distortion, the square root of the second invariant of the strain tensor is used (Groshong et al., 1984a; Ferrill, 1991). The twin strains calculated for the grains in the pore-filling cement of the host rocks are smaller than the strains calculated for the grains in the veins. The former range from 0.08 to 0.2 (average 0.15) and the latter from 0.11 to 3.61 (average 0.98). The twinned grains in both places have similar average sizes (401 μm vs 550 μm). The larger twin strain values in the veins suggest that the veins deformed more easily than the host rock. The maximum shortening values (percent elongation) are in the range from −0.045% to −3.8% (average −0.945%, Table 2). This range of magnitudes is smaller than those found in thin-skinned thrust belts (e.g. −3.6%, Groshong et al., 1984a; −4%, Holl and Anastasio, 1995) or fold–thrust belts (e.g. −1.9%, Ferrill, 1991). The plot of grain size vs twin density (twins/mm) shows that the twin density decreases with increasing grain size (Fig. 4a), i.e. twinning is grain-size dependent (Rowe and Rutter, 1990). However, the plot of grain size vs twin width (Fig. 4b) shows no systematic relationship.

The method used here allows us to calculate the orientations of the principal strain axes (e_1 , e_2 and e_3 , Fig. 5a–e). The analysis of the deformation history experienced by the microveins subsequent to their formation is described separately for each group of strain axis orientations, since each family probably corresponds to a different deformation episode. Assuming

equivalence between the stress and strain axes (e.g. $\sigma_1 \Leftrightarrow e_3$), the assumption of coaxiality is tested in each sample comparing the orientations of the principal axes of stress and strain.

The first group comprises the samples with approximately horizontal maximum shortening axes, i.e. related to compressional tectonic events. Four different subgroups have been established based on axes trends.

Subgroup 1—the maximum shortening axes are orientated consistently NW–SE and show gentle plunges. The trends of the maximum extension axes are NE–SW (Fig. 5a, samples N9a, N9b, N2, N10a and N7). The intermediate strain axes are orientated approximately vertically, except in the samples N10a and N7, which could result from later tilting or non-coaxial strain. These veins yield the maximum values of percent elongation. In the samples N9a, N9b and N2, the maximum extension axis is in the same orientation as the c -axes suggesting that twinning microstructures could be formed during vein formation. However, the samples N10a and N7 show an oblique angle between these two axes, suggesting that twinning could be later than the vein development. These samples show sub-horizontal orientations of σ_1 and σ_3 with NW–SE and NE–SW trends respectively, σ_1 is in the same orientation as e_3 suggesting that deformation occurred during the vein growth and under coaxial conditions. Assuming equivalence between the stress and strain axes, we have interpreted this entire group as veins

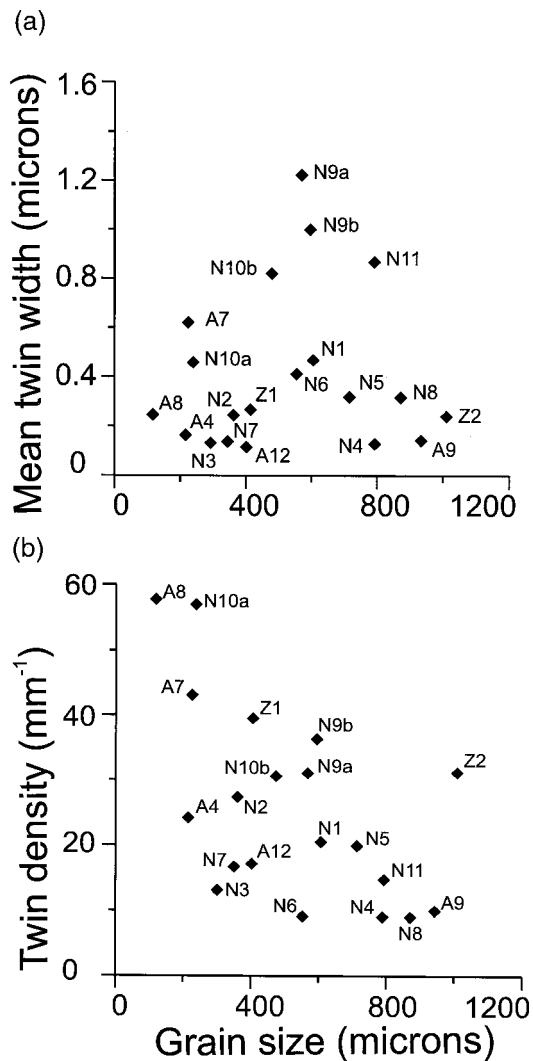


Fig. 4. Relationship between twins and grain size. (a) Grain size vs mean twin width. (b) Grain size vs twin density. The graph shows that twin density is grain size dependent.

grown and deformed during the Guadarrama Compression, and connected to this strike slip regime. Some of them (N10a and N7) could deform late with respect to the formation of the vein.

Subgroup 2—the maximum shortening axes tend to be N–S and nearly horizontal (Fig. 5b, samples N6, N4, N1 and N10b). The maximum extension axes are orientated E–W and the intermediate axis is nearly vertical in all samples of this group except in N10b. In most of the veins (N6, N1 and N10b) the maximum extension axes are not in the same orientation as the c -axes suggesting that twinning was formed after vein formation. The directions of σ_1 and e_3 are, in general, parallel. Consequently, a coaxial deformation can be deduced. The orientations of the calculated maximum shortening directions do not coincide with any of the principal compression directions described for the principal tectonic episodes of this chain. However, other

microstructures, such as stylolites (Fig. 7) clearly show this compression direction (e.g. Capote et al., 1982), which could be related to local deformation.

Subgroup 3—the orientation of strain axes in a small number of veins show subhorizontal maximum shortening axes with NE–SW-trends, and e_2 and e_3 axes with gentle to moderate plunges (Fig. 5c, samples N11, A9 and N8). In all the samples the c -axis maxima and the e_3 directions have the same orientations, then the twinning process is related with the vein formation episode. The deformation is coaxial, i.e. σ_1 and e_3 and σ_3 and e_1 have the same directions on samples N11 and A9. As this shortening direction is parallel to those of the Iberica Compression, the deformation is inferred to have occurred during this deformation episode.

Subgroup 4—samples A8, A4 and A12 (Fig. 5d) produce an E–W maximum shortening direction. In one vein (A8), the coaxial character of deformation together with their relationship with the vein development is clearly shown by the parallelism between the maximum shortening and extension axes, σ_1 and σ_3 and c -axis maxima. In the other two veins, these relationships are not so clearly observed, with the e_2 and e_3 axes being inclined. This E–W shortening is correlated to the Altomira tectonic event, and is consistent with the stylolite orientation (Fig. 7a).

The second group includes those samples that produce a nearly vertical maximum shortening axis and subhorizontal maximum extension (Fig. 5e, samples N3, Z1, A7, Z2 and N5); this strain is then correlated with regional extension. The orientation of the maximum compressive strain and σ_1 are only nearly parallel in samples N5 and A7, which suggests non-coaxial deformation. The maximum extension axes lie in a N–S or an E–W plane. These directions could be related with the final extensional episode of the Iberian Chain evolution or with local extensions (e.g. extensions in the outer arc of folds).

In summary, the calculated strain axis orientations correlate approximately, with the main tectonic events of this chain (Guadarrama, Iberica and Altomira) and probably, with the final extensional period. These shortening directions also correlated with the fold trends of this region (Fig. 1). A local episode of N–S maximum compressive strain is also established. This is the only episode where the vein development and the twinning process seem not to be simultaneous.

4.2. Twinning paleopiezometry

Estimates of differential stress magnitudes (paleopiezometry) using twins assume numerous restrictions (see the revision of Burkhard, 1993, and references therein), requiring that the samples consist of coarse grained

(a)

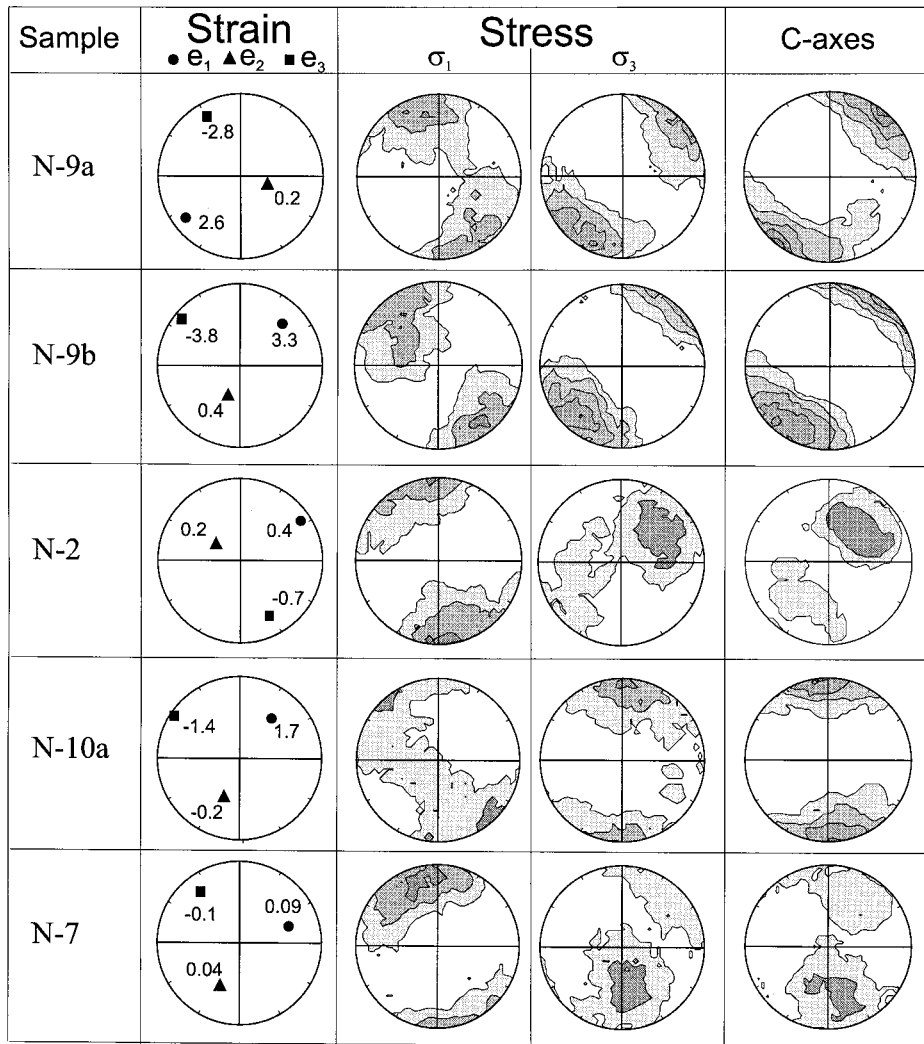
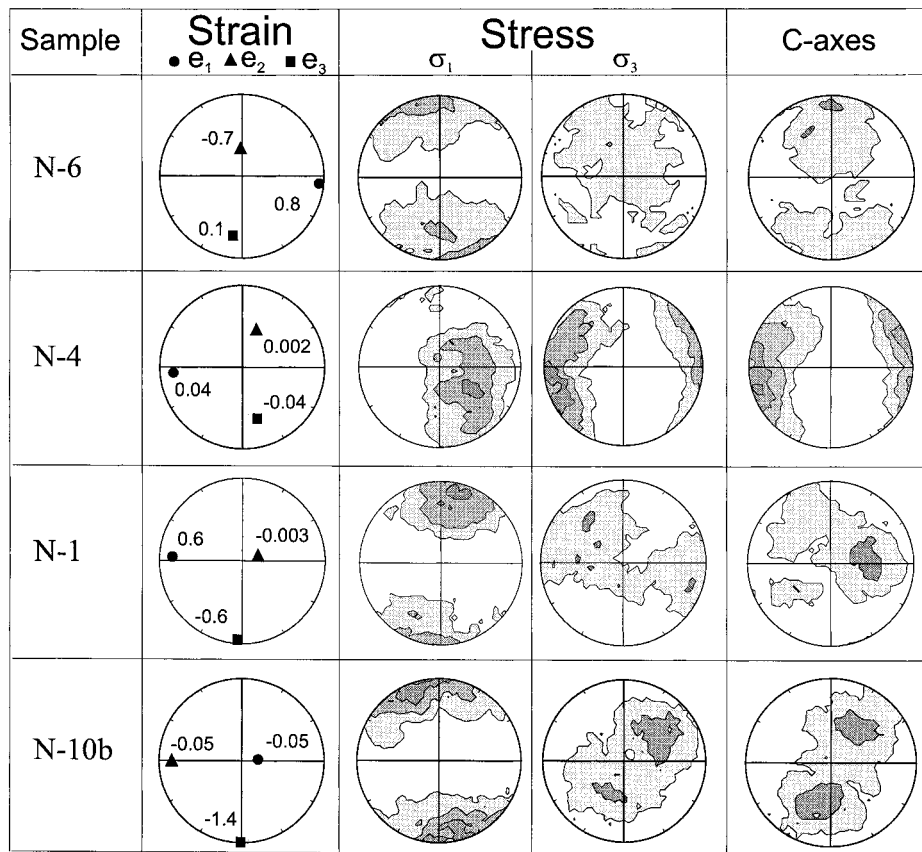


Fig. 5. Results of calcite twinning analysis. Stereographic plot of principal strain axes position, all strain results are given in percentage, shortening is negative. Density diagrams of σ_1 and σ_3 orientations and c -axis orientations (Schmidt projection, lower hemisphere, contour levels 1%). (a) Veins with e_3 axes orientated NW–SE. Guadarrama Compression. (b) Veins with e_3 axes orientated N–S. (c) Veins with e_3 axes orientated NE–SW. Iberica Compression. (d) Veins with e_3 axes orientated E–W. Altomira Compression. (e) Veins with e_3 axes orientated nearly vertical. Final extension.

(b)



(c)

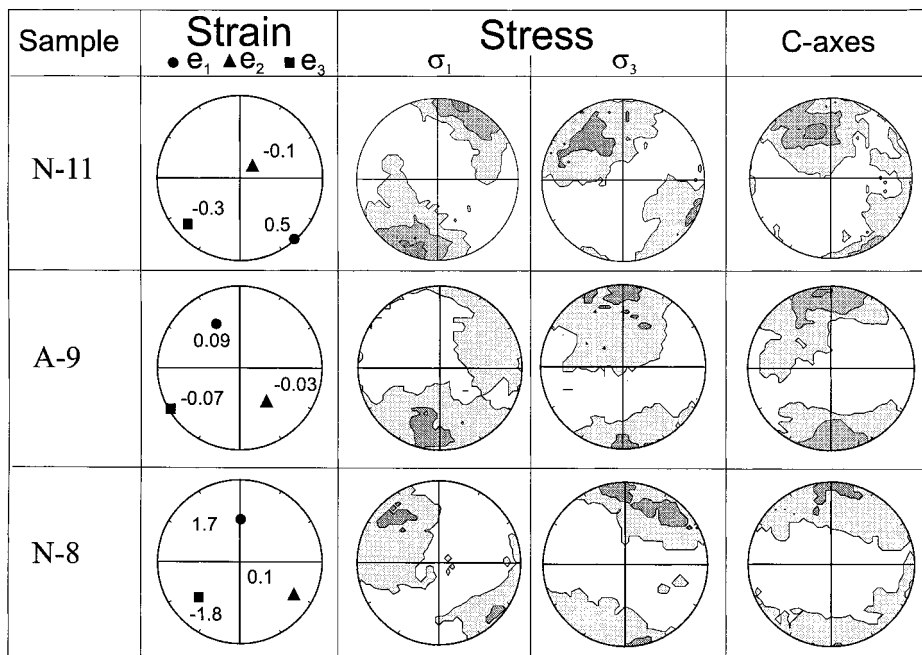
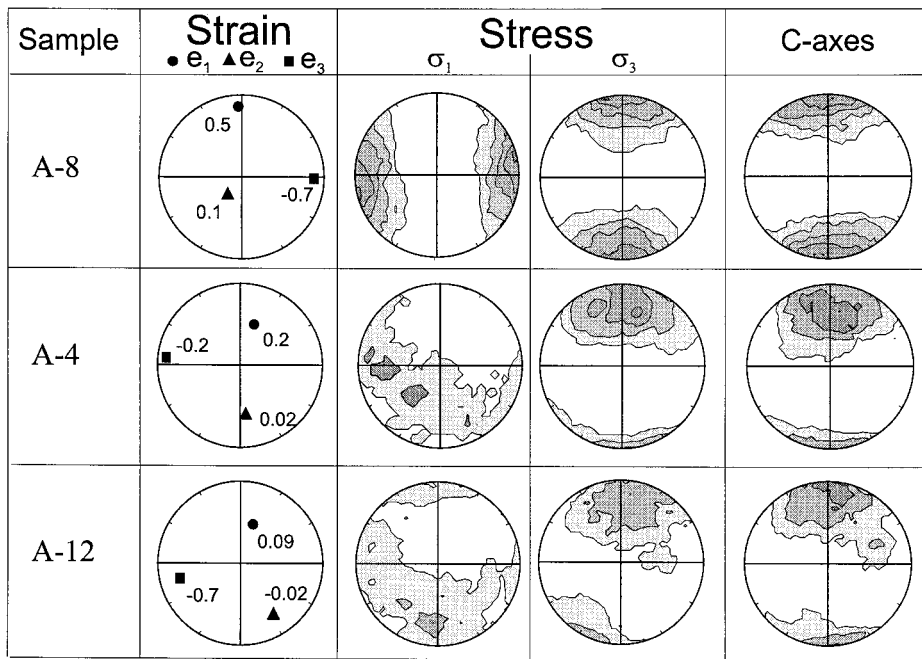


Fig. 5. (continued).

(d)



(e)

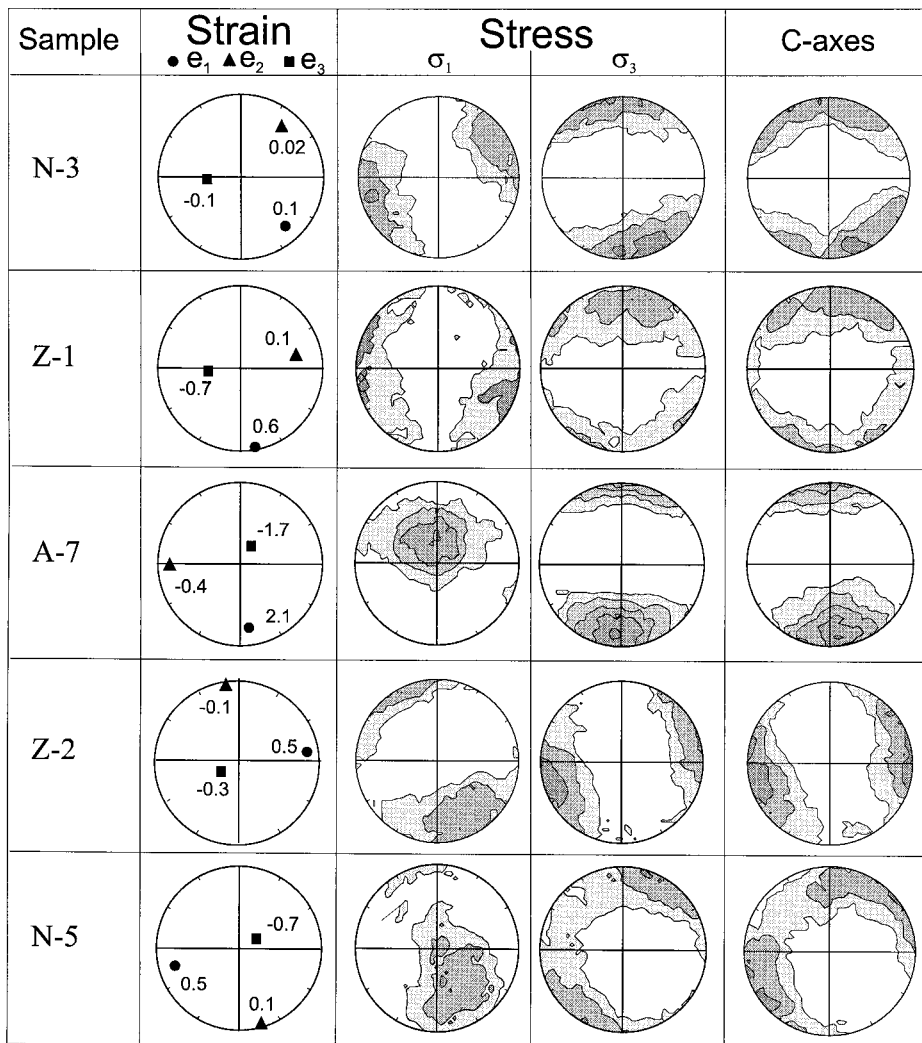


Fig. 5. (continued).

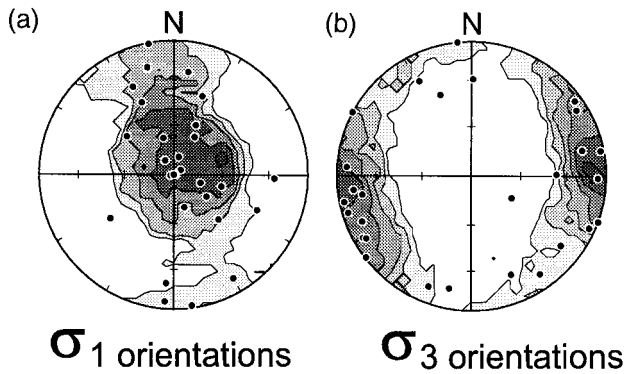


Fig. 6. Results of the striated-fault-plane analysis after the method of Reches (Reches, 1987). The points represent the calculated positions of σ_1 and σ_3 for the analysed data set. (Schmidt projection, lower hemisphere. Contour intervals 1%.)

calcite, were deformed at low temperature and suffered little deformation.

Recently, Ferrill (1998) has proposed that for limestones deformed at low temperatures the technique of Jamison and Spang (1976) yields the best estimations, although this approach has a severe limitation in the selected value for the critical resolved shear stress (τ_c) necessary for twinning. The value of 10 MPa proposed by Jamison and Spang has been controversial, but recently Lacombe and Laurent (1996) concluded that this value is reasonable.

In this region, the twinned crystals often display one (82.1%) or two (17.5%) sets of straight twins. Only a few grains exhibit three sets (0.4%). The results from applying the Jamison and Spang technique to these data yield differential stress magnitudes around 62 MPa (estimations were made using the percentage of grains with two sets of twins).

4.3. Fault population analysis

The results of the stress inversion method of Reches (1987) are summarised in Table 1 and plotted in Fig. 6. The main parameters of the calculated tensors are a mean coefficient of friction of 0.69 (close to Byerlee (1978) assumption: $\mu = 0.89$ when $3 < \sigma_n < 200$ MPa) and stress ratio value [$\phi = (\sigma_2 - \sigma_3)/(\sigma_1 - \sigma_3)$] between 0.02 and 0.69 (mean 0.33). The azimuths of σ_1 for the sample sites show a uniform NNW–SSE orientation, but they have two different plunges whereby they could be oriented subhorizontally or subvertically (Fig. 6a). The σ_3 axes are oriented subhorizontal and grouped in a single maximum with an ENE–WSW azimuth (Fig. 6b). These principal stress axis orientations are interpreted as the result of two deformation events having the same σ_3 orientations, but differently oriented σ_1 (and hence σ_2). The σ_1 orientations imply one strike-slip stress tensor (σ_1 and σ_3 near the hori-

zontal) and another extensional (σ_1 near the vertical and σ_3 horizontal). Field evidence, such as cross-cutting relationships of the faults, suggests that the normal faults are younger than the reverse and strike-slip faults. Moreover, in some fault planes, two striae are present with the steeply plunging striations being demonstrably later. The extensional tensor probably corresponds to the last tectonic event recorded by the faults in this area. The existence of only one extension direction is justified because many of the former strike-slip faults were reactivated as extensional features during the last deformation event.

The orientation of the strike-slip stress tensor implies a NNW–SSE maximum horizontal shortening direction, which corresponds with the established shortening direction of the third compressive event defined in this region (Guadarrama Compression, De Vicente, 1988; Capote et al., 1990) and fits well with the observed macrostructure, fault displacements and stylolite orientations (Capote et al., 1982).

4.4. Stylolites

In this region, many veins cut or are cut by stylolites, suggesting that these microstructures were developed more or less at the same time. The analysis of

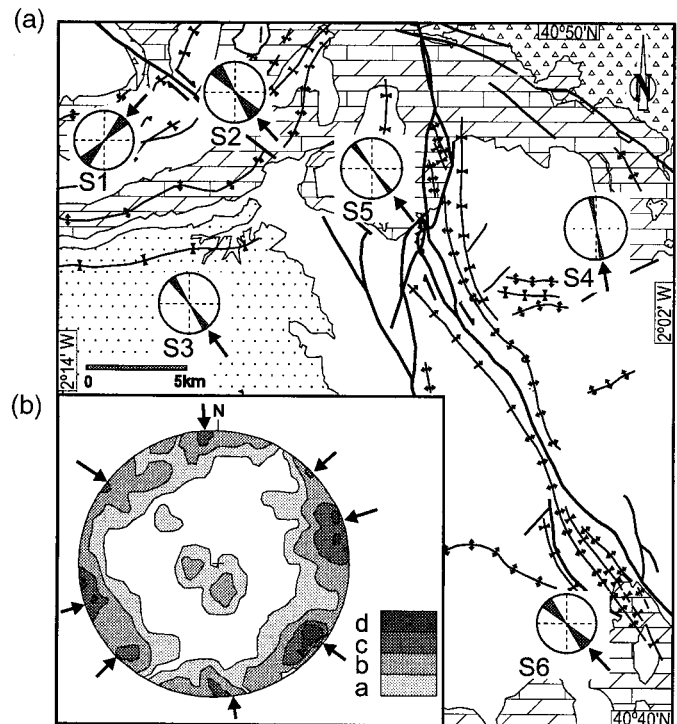


Fig. 7. Stylolite orientations. (a) Maximum shortening direction deduced from stylolites in the studied area. (b) Density diagrams of calculated e_3 positions from stylolitic peaks within the NW Iberian Chain (from Capote et al., 1982). Contour intervals, $a = 0.28\%$, $b = 1.38\%$, $c = 3.58\%$, $d = 5.23\%$.

stylolitic seam orientations (Fig. 7) yield three orientations of the maximum shortening, N–S (Fig. 7a, S4), NW–SE (Fig. 7a, S2, S3, S5 and S6) and NE–SW (Fig. 7a, S1). These directions have the same trends as those deduced from the twinning analysis, demonstrating their relationship. Previous studies of stylolites in this part of the Iberian Chain (e.g. Capote et al., 1982), have established the same orientations together with another oriented ENE–WSW (Fig. 7b). These authors also find vertical stylolite peaks that could have been formed during burial in response to lithostatic load, or also in response to tectonic extension. In conclusion, the calculated maximum shortening directions from stylolites correlated well with the strain axis orientations deduced from twinning in calcite veins.

5. Discussion and conclusion

Assuming the equivalence between the principal strains and stresses (i.e. an elastic analysis), the orientations of the principal strains give a complete description of the stress evolution of this region. The stress orientations are described in more detail in the twin analysis than using the results of fault population analysis. The strain axis orientations record a more detailed tectonic evolution, with the maximum shortening directions correlating to all the tectonic episodes previously described for this part of the Iberian Chain being observed. Two groups of deformations have been established, characterised by the vertical and horizontal orientation of the maximum shortening axis. In the former group four different trends are found: (1) A maximum shortening direction orientated NW–SE that is correlated with the Guadarrama compression. The number of samples that record this event and the strain magnitudes suggest that it is the most important in the structural development of this area. (2) A deformation episode where the maximum shortening direction is orientated N–S. (3) A NE–SW compression (Ibérica Compression). (4) An E–W compression that is recorded in a few samples. This latter episode is probably related to the Altomira Compression. (5) An extensional episode that is observed in several samples. In most of the samples, except in group 2, the twinning process took place in concert with the vein opening process. The e-twin analysis results clearly show that the late Mesozoic–Cenozoic evolution of this area has involved polyphase deformation. The low strain magnitudes that have been found correspond well with the moderate deformations that characterise this area of gentle folds. No significant differences between principal strain orientations deduced from grains of host rocks and veins

have been identified. However, the magnitudes of twin strain are higher in the veins than in the host rocks.

The comparison between the stress orientation determined from the fault analysis and those determined from the calcite e-twins is significant because fault planes can be reactivated by successive stress fields. The fault analysis results show that only a single direction of maximum horizontal extension (related to two different tectonic episodes) is recorded, while the mechanical twinning of calcite records a more detailed tectonic evolution, specifically the previously described extension directions inferred from all the tectonic episodes within this part of the Iberian Chain. Hence, the calcite twins record not only the same stress orientations as the faults, but also the previous deformation episodes. Stylolites show the same shortening directions as the microveins.

The results are consistent with independent stress–strain data, i.e. stylolites, faulting and major structure and a good correlation has been found between the orientations of principal strains deduced from the twinning analysis and the principal deformation events previously established for the Iberian Chain. Therefore, as has been previously noted (e.g. Lacombe et al., 1990; Rocher et al., 1996), these analyses can be used to extrapolate the interpretations of strains from grain-scale to regional-scale. Nevertheless, the possible spatial heterogeneities must be considered in light of the fact that some of the principal strain orientations established could be related with local heterogeneities.

Acknowledgements

The authors thank Dr M.A. Evans for allowing us to use their program of calcite e-twin analysis. Dr G. de Vicente, Dr A. Muñoz-Martín and Prof. R. Capote del Villar contributed many stimulating ideas and helped with the preparation of the figures. The manuscript was greatly improved by the review comment of Dr S. Covey-Crump and Prof. J.C. White. This work was financed by a D.G.I.C.Y.T. (Spain) research grant (PB94-0242).

References

- Adell, F., Lendínez, A., Martínez, F., Tena-Dávila, M., 1981. Mapa Geológico de España, Zaorejas, Instituto Geológico y Minero Mapa 513, scale 1:50,000.
- Alvaro, M., 1975. Estilolitos tectónicos y fases de plegamiento en el área de Sigüenza (borde del Sistema Central y de la Cordillera Ibérica). *Estudios Geológicos* 31, 241–247.
- Alvaro, M., Capote, R., Vegas, R., 1979. Un modelo de evolución geotectónica para la Cadena Celtibérica. *Acta Geológica Hispánica* 14, 241–247.
- Arthaud, F., Choukroune, P., 1972. Méthode d'analyse de la tectoni-

- que cassante à l'aide des microstructures dans les zones peu déformées. Example de la plate-forme Nord-Aquitaine. *Revue Institute Français du Pétrole* 27, 715–732.
- Bott, M.H.P., 1959. The mechanism of oblique-slip faulting. *Geological Magazine* 96, 109–117.
- Burkhard, M., 1993. Calcite twins, their geometry, appearance and significance as stress–strain markers and indicators of tectonic regime: a review. *Journal of Structural Geology* 15, 351–368.
- Byerlee, J., 1978. Friction of rocks. *Pure and Applied Geophysics* 116, 615–626.
- Calvo, J.P., Damms, R., Morales, J., López Martínez, N., Agustí, J., Anádon, P., Armenteros, I., Cabrera, L., Civis, J., Corrochano, A., Díaz Molina, M., Elizaga, E., Hoyos, M., Martín, M., Martínez, J., Moissenet, E., Muñoz, A., Pérez García, A., Pérez González, A., Portero, J.M., Robles, F., Santiesteban, C., Torres, T., Van der Meulen, A., Vera, J., Mein, P., 1993. Up-to-date Spanish continental Neogene synthesis and paleoclimatic interpretation. *Revista de la Sociedad Geológica de España* 6, 29–40.
- Capote, R., Díaz, M., Gabaldón, V., Gómez, J.J., Sánchez de la Torre, L., Ruiz, P., Rossel, J., Sopena, A., Yébenes, A., 1982. Evolución sedimentológica y tectónica del ciclo alpino en el tercio noroccidental de la Rama Castellana de la Cordillera Ibérica. *Temas Geológicos Mineros* 5, 1–290.
- Capote, R., De Vicente, G., González-Casado, J.M., 1990. Evolución de las deformaciones alpinas en el Sistema Central Español (S.C.E.). *Geogaceta* 7, 20–22.
- De Vicente, G., 1988. Análisis poblacional de fallas. El sector de enlace Sistema Central–Cordillera Ibérica. PhD thesis, Universidad Complutense de Madrid.
- De Vicente, G., González-Casado, J.M., Bergamin, J.F., Tejero, R., Babín, R., Rivas, A., Hernández-Henrile, J.L., Giner, J., Sánchez-Serrano, F., Muñoz, A., Villamor, P., 1992. Alpine structure of the Spanish Central System. Abstracts of proceedings. Universidad de Salamanca, Salamanca.
- De Vicente, G., Giner, J.L., Muñoz-Martín, A., González-Casado, J.M., Lindo, R., 1996. Determination of present-day stress tensor and neotectonic interval in the Spanish Central System and Madrid Basin, central Spain. *Tectonophysics* 266, 405–424.
- Evans, M.A., Groshong Jr., R.H., 1994. A computer program for the calcite strain-gauge technique. *Journal of Structural Geology* 16, 277–281.
- Ferrill, D.A., 1991. Calcite twin width and intensities as metamorphic indicators in natural low-temperature deformation of limestone. *Journal of Structural Geology* 13, 667–675.
- Ferrill, D.A., 1998. Critical re-evaluation of differential stress estimates from calcite twins in coarse-grained limestones. *Tectonophysics* 285, 77–86.
- Groshong Jr., R.H., 1972. Strain calculated from twinning in calcite. *Geological Society of America Bulletin* 83, 2025–2048.
- Groshong Jr., R.H., 1974. Experimental test of the least-squares strain gauge calculation using twinned calcite. *Geological Society of America Bulletin* 85, 1855–1864.
- Groshong Jr., R.H., 1988. Low temperature deformation mechanism and their interpretation. *Geological Society of America Bulletin* 100, 1329–1360.
- Groshong Jr., R.H., Pfiffner, O.A., Pringle, L.R., 1984a. Strain partitioning in the Helvetic thrust belt of eastern Switzerland from the leading edge to the internal zone. *Journal of Structural Geology* 6, 5–18.
- Groshong Jr., R.H., Teufel, L.W., Gasteiger, C., 1984b. Precision and accuracy of the calcite strain-gauge technique. *Geological Society of America Bulletin* 95, 357–363.
- Holl, J.E., Anastasio, D.J., 1995. Cleavage development within a foreland fold and thrust belt, southern Pyrenees, Spain. *Journal of Structural Geology* 17, 357–369.
- Jamison, W.R., Spang, J.H., 1976. Use of calcite twin lamellae to infer differential stress. *Geological Society of America Bulletin* 87, 868–872.
- Lacombe, O., Laurent, Ph., 1996. Determination of deviatoric stress tensors based on inversion of calcite twin data from experimentally deformed monophase samples: preliminary results. *Tectonophysics* 255, 189–202.
- Lacombe, O., Angelier, J., Laurent, Ph., Bergerat, F., Tournet, Ch., 1990. Joint analysis of calcite twins and faults slips as a key for deciphering polyphase tectonics: Burgundy as a case study. *Tectonophysics* 182, 279–300.
- Lacombe, O., Angelier, J., Laurent, Ph., 1992. Determining paleo-stress orientations from faults and calcite twins: a case study near the Sainte-Victoire Range (southern France). *Tectonophysics* 201, 141–156.
- Laurent, Ph., Bernard, Ph., Vasseur, G., Etchechopar, A., 1981. Stress tensor determination from the study of e-twins in calcite: a linear programming method. *Tectonophysics* 78, 651–660.
- Manera, A., 1981. Determinación de cuatro fases de deformación en el extremo suroccidental de la Sierra de Altomira. *Estudios Geológicos* 37, 233–243.
- Muñoz-Martín, A., 1997. Evolución geodinámica del borde oriental de la Cuenca del Tajo desde el Oligoceno hasta la actualidad. PhD thesis, Universidad Complutense de Madrid.
- Muñoz-Martín, A., De Vicente, G., González-Casado, J.M., 1994. Análisis tensorial de la deformación superpuesta en el límite oriental de la cuenca de Madrid. *Cuadernos do Laboratorio Xeológico de Laxe* 19, 203–214.
- Newman, J., 1994. The influence of grain size and grain size distribution on methods for estimating paleostresses from twinning in carbonates. *Journal of Structural Geology* 16, 1589–1601.
- Pfiffner, O.A., Burkhard, M., 1987. Determination of paleo-stress axes orientations from fault, twin and earthquake data. *Annales Tectonicae* 1, 48–57.
- Reches, Z., 1987. Determination of the tectonic stress tensor from slip along faults that obey the Coulomb yield condition. *Tectonics* 7, 849–861.
- Reches, Z., Baer, G., Hatzor, Y., 1992. Constraints on the strength of the upper crust from stress inversion of fault slip data. *Journal of Geophysical Research* 97, 12481–12493.
- Rocher, M., Lacombe, O., Angelier, J., 1996. Mechanical twin sets in calcite as markers of recent collisional events in a fold-and-thrust belt: Evidence from reefal limestones of south-western Taiwan. *Tectonics* 15, 984–996.
- Rodríguez-Pascua, M.A., 1993. Cinemática y dinámica de las deformaciones alpinas en la zona del Alto Tajo (Guadalajara). MS thesis, Universidad Complutense de Madrid.
- Rodríguez-Pascua, M.A., De Vicente, G., González-Casado, J.M., 1994. Cinemática y dinámica de las deformaciones en la zona del Alto Tajo (Guadalajara). *Cuadernos do Laboratorio Xeológico de Laxe* 19, 163–174.
- Rowe, K.J., Rutter, E.H., 1990. Paleostress estimation using calcite twinning: experimental calibration and application to nature. *Journal of Structural Geology* 12, 1–17.
- Salas, R., Casas, A., 1993. Mesozoic extensional tectonics, stratigraphy and crustal evolution during the Alpine cycle of the eastern Iberian Chain. *Tectonophysics* 228, 33–55.
- Sell, I., Poupeau, G., Casquet, C., Galindo, C., González-Casado, J.M., 1995. Exhumación alpina del bloque morfotectónico Pedriza–La Cabrera (Sierra del Guadarrama, S.C.E.): Potencialidad de la termocronometría por trazas de fisión en apatitos. *Geogaceta* 18, 23–26.
- Simón-Gómez, J.L., 1986. Analysis of a gradual change in stress regime (example from the eastern Iberian Chain, Spain). *Tectonophysics* 124, 37–53.
- Spang, J.H., 1972. Numerical method for dynamic analysis of calcite twin lamellae. *Geological Society of America Bulletin* 83, 467–472.

- Teufel, L.W., 1980. Strain analysis of superposed deformation using calcite twin lamellae. *Tectonophysics* 65, 291–309.
- Turner, F.J., 1953. Nature and dynamic interpretation of deformation lamellae in calcite of three marbles. *American Journal of Science* 251, 276–298.
- Turner, F.J., 1962. “Compression” and “tension” axes determined from [0112] twinning in calcite. *Journal of Geophysical Research* 67, 1660.
- Turner, F.J., Weiss, L.E., 1963. *Structural Analysis of Metamorphic Tectonites*. McGraw-Hill, New York.
- Vilas, L., Alonso, A., Arias, C., García, A., Mas, J.R., Rincón, R., Meléndez, N., 1983. The Cretaceous of the South-western Iberian Ranges (Spain). *Zittelania* 10, 245–254.
- Weiss, L.E., 1954. A study of tectonic style: Structural investigation of a marble quartzite complex in southern California. *University of California Publications in Geological Science* 30, 1–102.